1794 *Inorg. Chem.* **2010**, *49*, 1794–1800
DOI: 10.1021/ic9021596

Inorganic Chemistry
Article

Luminescence Change by the Solvent of Crystallization, Solvent Reorganization, and Vapochromism of Neutral Dicyanoruthenium(II) Complex in the Solid State

Taichi Abe,[†,§] Takayoshi Suzuki,[‡] and Kazuteru Shinozaki*[,†]

[†]*Department of Chemistry, Graduate School of Integrated Sciences, Yokohama City University, 22-2 Seto, Yokohama, 236-0027 Japan, and* [‡]*Department of Chemistry, Faculty of Science, Okayama University, 331 Tsushimanaka, Okayama 700-8530, Japan.* [§]*Present address: National Institute of Advanced Industrial Science and Technology (AIST), 111 Higashi, Tsukuba, Ibaraki 305-8565, Japan.*

Received November 2, 2009

The "solvent effect" on the solid-state luminescence of a neutral complex, $[Ru(dbb)_2(CN)_2]$ (dbb = 4,4′-di-*tert*-butyl-2,2′-bipyridine), was presented. The crystals of this complex showed a variety of luminescence color from orange to dark-red, depending on the acceptor number of the solvent included in the crystal as a solvent of crystallization. The luminescence change was very similar to the solvatochromism in solution, which was attributed to the local donor−acceptor interaction between the CN group and the solvent molecules. The dynamic shift observed in the transient emission spectrum of the crystalline powder was accounted for by the solvent molecule reorganization. X-ray crystallography of $[Ru(dbb)_2(CN)_2]\cdot 3(CH_3)_2CO$ showed the complex molecule having an approximate C_2 symmetry and very weak interactions between the acetone molecules and the CN groups. A three-dimensional network constructed by acetone molecules was observed in the hydrophobic space consisting of *t*-butyl groups in dbb ligands. A thin film of the complex showed vapochromic behavior such that the luminescence changed depending on the solvent of crystallization. This suggests a capability for organic molecule discrimination using the complex in the solid state.

Introduction

Luminescence of transition-metal complexes have been actively studied for the practical use of phosphorescent materials for light-emitting devices (OLEDs).[1−3] Since the complexes are used in a luminescent layer, the basic research and data accumulation of excited-state properties are necessary for the durability or the improvement of brightness for OLED. Recently, inorganic and material chemists have been fascinated by the luminescence of Pt(II) complexes in the solid state, especially the bright luminescence and vapochromism, which is the luminescence color change by exposure to organic solvent vapor.[4−9] The structural change induced by the sorption of an organic molecule into a crystal lattice causes the drastic luminescence color change. Similar chromisms induced by the change in crystal structure have been found for other metal complexes as well.[10−13] Recently, we reported the mechanochromism for Pt(5dpb)Cl (5dpbH = 1,3-di(5-methyl-2-pyridyl)benzene), of which luminescence color changed from yellow to orange by mechanical grinding.[14] The yellow and orange luminescence were very similar to the monomer and excimer emission in solution, respectively. For Ru(II) complexes, which had been most intensely studied among the transition-metal complexes in terms of the photoexcited properties, the vapochromism was observed as well. An anion complex, $(PPN)_2[Ru(bpy)(CN)_4]$ (PPN = bis(triphenylphosphine)iminium ion, bpy = 2,2′-bipyridine)[13] and a neutral complex, $[Ru(dbb)_2(CN)_2]$ (dbb = 4,4′-di-*tert*-butyl-2,2′-bipyridine),[15] were reported to show

*To whom correspondence should be addressed. E-mail: shino@yokohama-cu.ac.jp.

(1) Sun, Y.; Giebrink, N. C.; Noel, C.; Kanno, H.; Ma, B.; Thompson, M. E.; Forrest, S. R. *Nature* **2006**, *440*, 908.
(2) Baldo, M. A.; Thompson, M. E.; Forrest, S. R. *Nature* **2000**, *403*, 750.
(3) Baldo, M. A.; O'Brien, D. F.; You, Y.; Shoustikov, A.; Sibley, S.; Thompson, M. E.; Forrest, S. R. *Nature* **1998**, *395*, 151.
(4) Kato, M.; Omura, A.; Toshikawa, A.; Kishi, S.; Sugimoto, Y. *Angew. Chem., Int. Ed.* **2002**, *41*, 3183.
(5) Kato, M. *Bull. Chem. Soc. Jpn.* **2007**, *80*, 287.
(6) Buss, C. E.; Mann, K. R. *J. Am. Chem. Soc.* **2002**, *124*, 1031.
(7) Drew, S. M.; Janzen, D. E.; Buss, C. E.; MacEwan, D. I.; Dublin, K. M.; Mann, K. R. *J. Am. Chem. Soc.* **2001**, *123*, 8414.
(8) Grate, J. W.; Moore, L. K.; Janzen, D. E.; Veltkamp, D. J.; Kaganove, S.; Drew, S. M.; Mann, K. R. *Chem. Mater.* **2002**, *14*, 1058.
(9) Grove, L. J.; Rennekamp, J. M.; Jude, H.; Connick, W. B. *J. Am. Chem. Soc.* **2004**, *126*, 1594.
(10) Fernández, E. J.; López-de-Luzuriaga, J. M.; Monge, M.; Olmos, M. E.; Pérez, J.; Laguna, A.; Mohamed, A. A.; Fackler, J. P., Jr. *J. Am. Chem. Soc.* **2003**, *125*, 2022.
(11) Fernández, E. J.; López-de-Luzuriaga, J. M.; Monge, M.; Montiel, M.; Olmos, M. E.; Pérez, J.; Laguna, A.; Mendizabal, F.; Mohamed, A. A.; Fackler, J. P., Jr. *Inorg. Chem.* **2004**, *43*, 3573.
(12) Cariati, E.; Bu, X.; Ford, P. C. *Chem. Mater.* **2000**, *12*, 3385.
(13) Evju, J. K.; Mann, K. R. *Chem. Mater.* **1999**, *11*, 1425.
(14) Abe, T.; Itakura, T.; Ikeda, N.; Shinozaki, K. *Dalton Trans.* **2009**, 711.
(15) Abe, T.; Shinozaki, K. *Inorg. Chem.* **2005**, *44*, 849.

 Published on Web 01/20/2010

luminescence color change by exposure to moisture. In this work, for the neutral complex, it is presented that the vapochromism is observed for organic solvent vapors as well as moisture, and the luminescence color depends on the identity of the solvent vapor. The "solvent effect" on emission properties of the $[Ru(dbb)_2(CN)_2]\cdot n$(solvent) crystal is similar to that of the solution sample. The effect of solvent of crystallization is discussed in terms of the local donor−acceptor interaction and the solvent reorganization.

Experimental Section

Materials. $[Ru(dbb)_2(CN)_2]$ (dbb = 4,4′-di-*tert*-butyl-2,2′-bipyridine) was prepared according to the procedure previously reported.[15] The solid and solution samples were degassed in a vacuum line just before luminescence measurements. The solvents used for luminescence measurements were dried on molecular sieves, which were activated by evacuating and heating at 180 °C. The samples for ^{1}H NMR measurement were prepared in the vacuum line to prevent the contamination of water.

Measurements. UV−vis spectra were measured by a Shimazu MultiSpec 1500 spectrophotometer. FTIR spectra were measured by a Bruker IFS 66/V, and ^{1}H NMR spectra were taken by a JEOL NMX 270. Luminescence spectra and lifetimes were measured by a JASCO FP-6500 fluorescence spectrophotometer and a UNISOKU Nd:YAG laser photolysis system, respectively.

Crystallographic Studies. Single crystals of $[Ru(dbb)_2(CN)_2]\cdot n(CH_3)_2CO$ ($n = 3-4$) were grown by direct diffusion of *n*-hexane into a dilute acetone solution of the complex. A suitable crystal was mounted with a cryoloop and flash-cooled by a cold nitrogen stream. The X-ray diffraction data were obtained at −80(2)°C on a Rigaku R-axis rapid imaging plate detector with a graphite-monochromated Mo K_α radiation (λ = 0.71073 Å). Data were processed by the Process-Auto program package,[16] and absorption corrections were applied by the numerical method.[17] The structure was solved by the direct method using SIR 2004[18] and refined on F^2 (with all independent reflections) using the SHELXL97 program.[19] All non-H atoms were refined anisotropically, and H atoms were introduced at the positions calculated theoretically and treated with riding models. All calculations were carried out using the CrystalStructure software package.[20] In an asymmetric unit, there were four possible positions for acetones of crystallization; two of them are fully occupied, but the other two had fewer electron densities than those expected. Thus, we assumed a partial occupation (0.5) for these molecules; this assumption made their thermal parameters to be acceptable values. Crystal data are collected in Table 1, and selected bond lengths and angles are listed in Table 2.

Table 1. Crystallographic Data of $[Ru(dbb)_2(CN)_2]\cdot 3(CH_3)_2CO$

	$[Ru(dbb)_2(CN)_2]\cdot 3(CH_3)_2CO$
chemical formula	$C_{47}H_{66}N_6O_3Ru$
fw, g/mol	864.13
cryst. size (mm)	0.30 × 0.25 × 0.20
cryst. syst.	orthorhombic
space group	$P2_12_12_1$
a, Å	18.5622(5)
b, Å	15.5319(5)
c, Å	18.0697(6)
α, deg	90
β, deg	90
γ, deg	90
V, Å^3	5209.6(3)
Z	4
$\rho_{calcd.}$ g/cm^3	1.102
temp, K	193(2)
μ, mm^{-1}	0.346
λ(Mo Kα), Å	0.71075
θ range, deg	3.06−27.48
no. independent reflns	11 904
no. params	551
$R1(F^2)$ $[F_o^2 > 2\sigma(F_o^2)]^a$	0.046
$wR2(F^2)$ (all data)^b	0.119

^{a} $R1 = \sum||F_o| - |F_c||/\sum|F_o|$. ^{b} $wR2 = [\sum w(F_o^2 - F_c^2)^2/\sum wF_o^2]^{1/2}$.

Table 2. Selected Bond Lengths (Å) and Angles (deg) of $[Ru(dbb)_2(CN)_2]\cdot 3(CH_3)_2CO$

Ru−N(3)	2.054(3)	C(1)−Ru−C(2)	92.78(15)
Ru−N(4)	2.103(3)	N(1)−C(1)−Ru	173.9(4)
Ru−N(5)	2.095(3)	N(2)−C(2)−Ru	176.1(3)
Ru−N(6)	2.053(3)	C(1)−Ru−N(4)	171.31(13)
Ru−C(1)	2.004(3)	N(3)−Ru−N(4)	77.79(11)
Ru−C(2)	2.004(4)	N(5)−Ru−N(6)	77.65(12)
C(1)−N(1)	1.157(5)	C(2)−Ru−N(5)	172.55(14)
C(2)−N(2)	1.161(5)	N(3)−Ru−N(6)	172.38(12)

Results and Discussion

$[Ru(dbb)_2(CN)_2]$ crystal crystallized from an organic solvent contained the solvent molecule and showed a solvent-dependent color such as orange (methanol), red (acetone), and dark-red (benzene). The solvents used for the crystallization were dried on molecular sieves to prevent the contamination of water, and the crystallization was carried out in the dry atmosphere using a glovebox. If the solvent was wet, the crystal contained water molecules as a solvent of crystallization. Namely, the crystallization from water and wet chloroform gave orange crystals of $[Ru(dbb)_2(CN)_2]\cdot 2H_2O$ and red crystals of $[Ru(dbb)_2(CN)_2]\cdot H_2O$, respectively.[15] In the dry organic solvent system, ^{1}H NMR spectrum for any complex crystal dissolved in dry deuterated solvent clearly showed the presence of organic solvents of crystallization and the absence of water molecules.

In solution, the complex color arising from the metal-to-ligand charge transfer (MLCT) transition from Ru to dbb was strongly dependent on solvent.[21,22] The solvent effect of UV−vis absorption spectrum in solution was analyzed by the Onsager reaction field approach using the dielectric continuum model, where the complex was regarded as a point dipole in a cavity floating in the dielectric continuum with a dielectric constant *D*.[23−28] However, the MLCT energy had

(16) *PROCESS-AUTO. Automatic Data Acquisition and Processing Package for Imaging Plate Diffractometer*; Rigaku Corporation: Tokyo, Japan, **1998**.
(17) Higashi, T. *Shape, Program for Absorption*. Rigaku Corporation: Tokyo, Japan, **1999**.
(18) Burla, M. C.; Caliandro, R.; Camalli, M.; Carrozzini, B.; Cascarano, G. L.; De Caro, L.; Giacovazzo, C.; Polidori, G.; Apagna, R. *J. Appl. Crystallogr*. **2005**, *38*, 381.
(19) Scheldrick, G. M. *Acta Crystallogr., Sect. A: Fundam. Crystallogr*. **2008**, *64*, 112.
(20) *CrystalStructure, Crystal Structure Analysis Package*, version 3.7.0; Rigaku and Rigaku/MSC: The Woodlands, TX, **2000−2005**.
(21) Encinas, S.; Farran Morales, A.; Barigelletti, F.; Barthram, A. M.; White, C. M.; Couchman, S. M.; Jeffery, J. C.; Ward, M. D.; Grills, D. C.; George, M. W. *J. Chem. Soc., Dalton Trans*. **2001**, 3312.
(22) Simpson, N. R. M.; Ward, M. D.; Farran Morales, A.; Barigelletti, F. *J. Chem. Soc., Dalton Trans*. **2002**, 2449.
(23) Onsager, L. *J. Am. Chem. Soc*. **1936**, *58*, 1486.
(24) Lippert, E. *Z. Naturforsch* **1955**, *10a*, 541.
(25) Mataga, N.; Kaifu, M.; Koizumi, M. *Bull. Chem. Soc. Jpn*. **1956**, *29*, 465.
(26) Kober, E. M.; Sullivan, B. P.; Meyer, T. J. *Inorg. Chem*. **1984**, *23*, 2098.
(27) Brunschwig, B. S.; Ehrenson, S.; Sutin, N. *J. Phys. Chem*. **1987**, *91*, 4714.
(28) Shinozaki, K; Kaizu, Y. *Bull. Chem. Soc. Jpn*. **1994**, *67*, 2314.

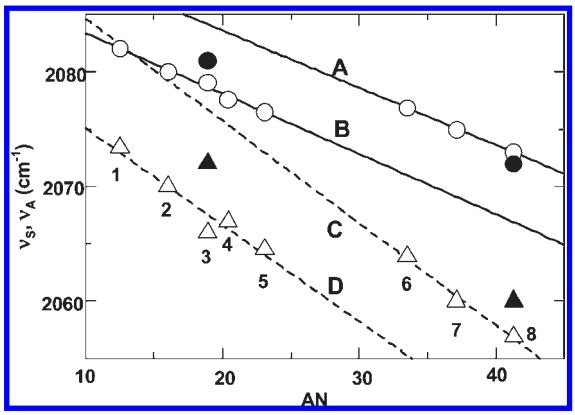

Figure 1. Plots of CN stretching frequencies of $[Ru(dbb)_2(CN)_2]$ vs AN of solvent: 1, acetone; 2, dimethylformamide; 3, acetonitrile; 4, dichloromethane; 5, chloroform; 6, 1-propanol; 7, ethanol; and 8, methanol. Open circles and triangles denote the symmetric (ν_S) and anti-symmetric (ν_A) frequencies, respectively, in solution. Filled circles and triangles denote those in the solid state. For aprotic solvents (1−5), the linear correlations between ν and AN, shown as lines **B** and **D**, are ν_S (cm^{-1}) = 2089−0.527 AN with $R^2 = 0.984$ and ν_A (cm^{-1}) = 2083−0.842 AN with $R^2 = 0.936$, respectively. For protic solvents (6−8), the line **A** and **C** are ν_S (cm^{-1}) = 2093−0.499 AN with $R^2 = 0.998$ and ν_A (cm^{-1}) = 2094−0.893 AN with $R^2 = 0.988$, respectively.

a poor correlation to $(1 - D)/(2D + 1)$ due to the local donor−acceptor interaction between the CN group and the solvent molecule. Instead, a plot of the MLCT energy (ν_{abs}) vs the acceptor number (AN), which was a measure of Lewis acidity of the solvent, showed a good correlation. A related complex, $[Ru(bpy)_2(CN)_2]$ (bpy = 2,2′-bipyridine), also showed a good linear relationship between the absorption maximum and the solvent AN.[29]

$[Ru(dbb)_2(CN)_2]$ in solution exhibited two strong infrared absorption bands at around 2000 cm^{-1} in the FTIR spectrum, which were assigned as the symmetric (ν_S) and anti-symmetric (ν_A) stretching modes of the CN ligands. The CN vibrational frequencies observed in several solvents were plotted against the AN. As shown in Figure 1, ν_S and ν_A were decreased in frequency with an increasing AN. For example, ν_S and ν_A were 2082 and 2073 cm^{-1} in acetone (AN 12.5), respectively, and 2077 and 2065 cm^{-1} in chloroform (AN 23.1). The local interaction between the CN ligand and the solvent enhances the Ru−CN back-donation, resulting in the decrease of the C−N bond order. The AN dependence observed in protic solvents seems to be different from that in the aprotic solvent. For example, the frequencies in chloroform (ν_S = 2076.5 and ν_A = 2064.5 cm^{-1}) are similar to those in 1-propanol (ν_S = 2076.9 and ν_A = 2063.9 cm^{-1}), despite the fact that the AN of chloroform (23.1) is much smaller than that of 1-propanol (33.5). Each ν_S in aprotic and protic solvents individually shows a good linear correlation to AN and so does ν_A.[30] The hydrogen bonding in protic solvents seems to result in a high-frequency shift from that which would be expected from the AN dependence in aprotic solvents. This is consistent with the high-frequency shift due to the protonation of the CN ligand.[15] The CN frequencies of the $[Ru(dbb)_2(CN)_2]$ crystal with no entrained solvent molecules were observed at ν_S = 2077 and ν_A = 2066 cm^{-1},[15] which were coincident with those in chloroform and 1-propanol. The frequencies (ν_S = 2072 and ν_A = 2060 cm^{-1}) of the $[Ru(dbb)_2(CN)_2]\cdot n CH_3OH$ crystal were smaller than those of the dry $[Ru(dbb)_2(CN)_2]$, whereas those (ν_S = 2081 and ν_A = 2072 cm^{-1}) of $[Ru(dbb)_2(CN)_2]\cdot n' CH_3CN$ were larger. In Figure 1, ν_S and ν_A are plotted against AN of the solvent of crystallization as filled circles and triangles, respectively. The results for the crystal samples are in good agreement with those in solution. The solvent of crystallization seems to gives rise to a donor−acceptor interaction with the CN ligands similar to the case found in a fluid solution.

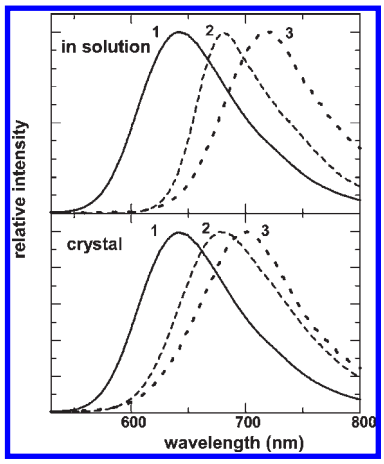

Figure 2. Emission spectra of $[Ru(dbb)_2(CN)_2]$ in solution and in the solid state with solvent of crystallization: 1, methanol; 2, acetonitrile; and 3, benzene.

The complex crystals showed various luminescence colors from bright-orange to dark-red, depending on the solvent of crystallization. For example, $[Ru(dbb)_2(CN)_2]\cdot n CH_3OH$, $[Ru(dbb)_2(CN)_2]\cdot n' CH_3CN$, and $[Ru(dbb)_2(CN)_2]\cdot n'' C_6H_6$ emitted an orange-red luminescence, peaking at 640, 678, 700 nm, respectively. Figure 2 shows the emission spectra of $[Ru(dbb)_2(CN)_2]\cdot n CH_3OH$, $[Ru(dbb)_2(CN)_2]\cdot n' CH_3CN$, and $[Ru(dbb)_2(CN)_2]\cdot n'' C_6H_6$ accompanying those of solution samples. The emission spectra of the complex crystals are similar to those in solution, and there is a resemblance in luminescence "solvent effect" between the crystal and solution samples. According to the previous analysis of solvent effects on emission spectra for $[Ru(bpy)_2(CN)_2]$ in solution,[29,31] the emission energy (ν_{em}) is plotted against the AN of the solvent in Figure 3. Open and filled circles correspond to the emission maxima ν_{em}'s of the solution and the solid samples, respectively, and squares are absorption maximum (ν_{abs}'s) of the solution sample. A linear correlation between ν_{em} of the crystal samples with the AN is observed, and moreover, the plots for the crystal and solution samples are coincident with each other. It is clearly shown that the effect of the solvent of crystallization on the solid-state emission is very similar to that of the solvent effect in solution. The solvent contribution to the MLCT transition energy is dominated by the local donor−acceptor interaction, according to the literature.[29,32]

(29) Timpson, C. J.; Bignozzi, C. A.; Sullivan, B. P.; Kober, E. M.; Meyer, T. J. *J. Phys. Chem.* **1996**, *100*, 2915.

(30) For ν_S, the slopes are evaluated as −0.499 and −0.527 for protic and aprotic solvents, respectively, and the intercepts are 2093 cm^{-1} and 2088 cm^{-1}. The correlation coefficients are r^2 = 0.998 and 0.984 for protic and aprotic solvents, respectively. For ν_A, the slopes are evaluated as −0.893 and −0.842 for protic and aprotic solvents, respectively, and the intercepts are 2094 cm^{-1} and 2083 cm^{-1}. The correlation coefficients are r^2 = 0.988 and 0.936 for protic and aprotic solvents, respectively.

(31) Fung, E. Y.; Chua, A. C. M.; Curtis, J. C. *Inorg. Chem.* **1988**, *28*, 1294.

(32) Curtis, J. C.; Sullivan, B. P.; Meyer, T. J. *Inorg. Chem.* **1983**, *22*, 224.

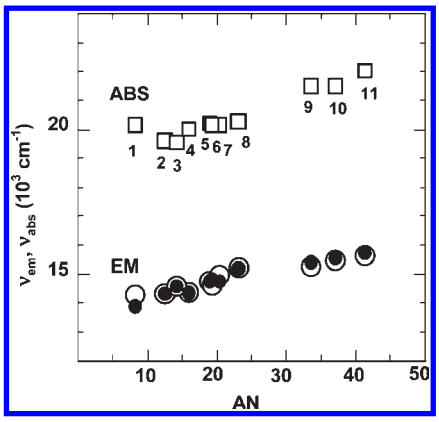

Figure 3. Plots of luminescence peak (ν_{em} in cm^{-1}) vs solvent acceptor number (AN) for $[Ru(dbb)_2(CN)_2]$ in solution (○) and in the solid−state (●): 1, benzene; 2, acetone; 3, pyridine; 4, dimethylformamide; 5, acetonitrile; 6, dimethylsulfoxide; 7, dichloromethane; 8, chloroform; 9, 1-propanol; 10, ethanol; and 11, methanol. Absorption peak (ν_{abs} in cm^{-1}) in solution is also plotted as □.

As the enhancement of the donor−acceptor interaction at the CN ligands stabilizes the d_π (Ru) orbitals in energy due to the increased π-backbonding to CN, the MLCT emission is blue-shifted in solvents with a high AN. The linear correlation between the ν_{abs} and the AN also clearly indicates the local interaction between the solvent and the CN ligands.

X-ray crystallography performed on a red crystal of $[Ru(dbb)_2(CN)_2]$ including acetone molecules revealed the molecular structure of the Ru(II) complex and the solvent organization in the crystal. The complex molecule has an approximately C_2 symmetry, and there are four possible positions for the acetone molecules, as shown in Figure 4. Selected bond lengths and angles are listed in Table 2. The bond lengths of Ru−N3 and Ru−N6 are 2.054(3) and 2.053(3) Å, respectively, and are very similar to those of $[Ru(bpy)_3]^{2+}$ (2.056 Å).[33] On the other hand, those of Ru−N4 (2.095(3) Å) and Ru−N5 (2.103(3) Å) are longer because of the strong trans influence of the CN ligands. The result is in good agreement with 2.116 and 2.102 Å for Ru−N in $[Ru(bpy)(CN)_4]^{2-}$.[8] Both bond lengths of Ru−C1 and Ru−C2 are 2.004 Å and are, thus, nearly the same as the known 2.000 Å of $[Ru(bpy)(CN)_4]^{2-}$.[34] The bond lengths of C1−N1 and C2−N2 are 1.161(5) and 1.157(5) Å, respectively, which are similar to those of $[Ru(bpy)(CN)_4]^{2-}$ (1.142 Å), HCN (1.156 Å), and CN^- ion (1.16 Å).[35]

The red crystals of $[Ru(dbb)_2(CN)_2]\cdot n(CH_3)_2CO$ were found to effloresce easily by the release of acetone molecules, and the crystal used for the diffraction study seemed to be partially effluorescent. Among four possible acetone molecules, **A**−**D** in Figure 4, the acetone molecules **B** and **D** were assumed to be partially occupied (occupancy factors 0.5) because the thermal parameters for the atoms were unusually large if a full occupation for these atoms was postulated. Thus, we analyzed the structure under the assumption of n = 3. In the crystal structure, all acetone molecules are close to the hydrophobic dbb ligands, and the closest contact distances are C41···C9 = 4.015 Å for **A**, C26···O3 = 3.845 Å for **B**, C11···O2 = 3.267 Å for **C**, and C32···O4 = 3.969 Å for **D**. The acetone **C** is also close to the next Ru complex and stays at the pseudo-C_2 axis of the complex. The distances between the N atoms in CN groups and the C atom (>C═O) in the acetone are evaluated to be N1−C42 = 3.826 and N2−C42 = 4.807 Å. The N−O (>C═O) distances are N1−O2 = 4.662 and N2−O2 = 5.293 Å. The donor−acceptor interaction between the lone pair of the N atom in the CN ligand and the lowest π^* orbital of acetone is assumed to be very small. This result is consistent with the low acidity of acetone (AN = 12.5). Figure 5 shows the acetone molecule network surrounding the Ru complexes as a space filling model. It is clear that the acetone molecules are stored in the hydrophobic space constructed with *t*-butyl groups in ligands.

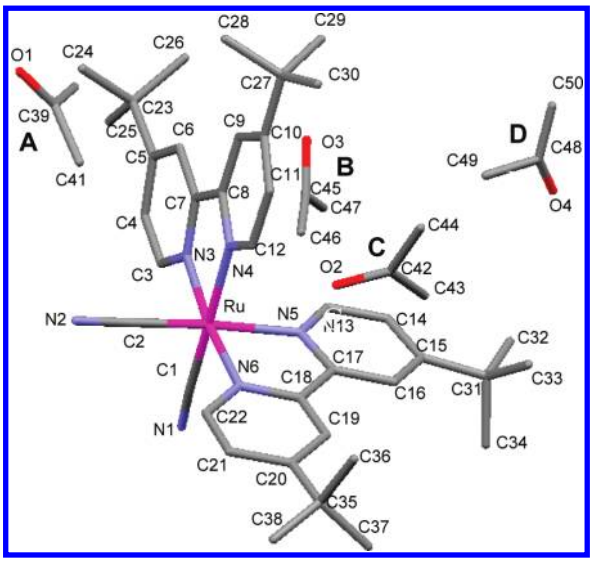

Figure 4. $[Ru(dbb)_2(CN)_2]$ and acetone molecules (**A**−**D**). For clarity, H atoms are hidden. The acetone molecules are close to the hydrophobic dbb ligands; the distances are: r(C41···C9) = 4.015 Å for **A**, r(C26···O3) = 3.845 Å for **B**, r(C11···O2) = 3.267 Å for **C**, and r(C32···O4) = 3.969 Å for **D**. Moreover, the acetone **C** is close to the CN ligands of the next Ru complex not shown and stays on the pseudo−C_2 axis of the complex. The distances between the N atoms of the CN ligands and the C atom of acetone C42 are r(N1···C42) = 3.826 and r(N2···C42) = 4.807 Å. The acetone molecules **B** and **D** are partially occupied (occupancy factors 0.5), presumably because they are easily released from the crystal.

Figure 6a shows time-resolved emission spectra of powdery $[Ru(dbb)_2(CN)_2]\cdot n CH_3OH$ at 77K, where the peak intensity in each spectrum is normalized to unity. The spectrum at 50 ns after a laser pulse excitation is peaking at 16 060 cm^{-1}, which is slightly blue-shifted from the steady-state emission (ν_{max} = 16 000 cm^{-1}). The peak shifts to a lower energy region with time and reaches 15 670 cm^{-1} at 2 000 ns. If the crystal is inhomogeneous due to the partial release of methanol, the emission spectrum would be a superposition of those of the Ru complexes surrounded by a variety of numbers of methanol molecules. In this case, the emission peaking at a higher energy should be long-lived compared with the lower energy emission, according to the energy gap law.[31] However, the result is opposite; that is, the emission peaking at 16 060 cm^{-1} has a shorter lifetime than that at 15 670 cm^{-1}. Therefore, we suggest that there is an energetic relaxation process in the excited state. This can be attributed to a "solvent reorganizational" relaxation in the photorelaxation process because this dynamic evident

(33) Rillema, D. P.; Jones, D. S.; Woods, C.; Levy, H. A. *Inorg. Chem.* **1992**, *31*, 2935.
(34) The bond length was obtained from the average of bond lengths 1.989 and 2.011Å for the equatorial CN ligands of $[Ru(bpy)(CN)_4]^{2-}$.
(35) Greewood, N. N.; Earnshaw, A. *Chemistry of the Elements*, 2nd ed. Elsevier Butterworth Heinemann: Jordan Hill, Oxford, 2005.

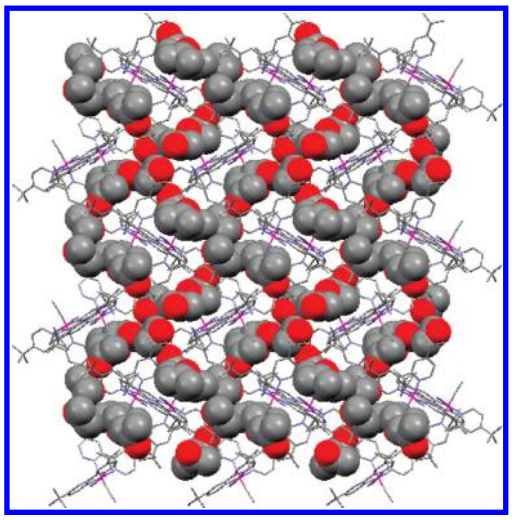

Figure 5. The acetone network represented by the space filling model in the $[Ru(dbb)_2(CN)_2]\cdot 3(CH_3)_2CO$ crystal. The red spheres are the O atoms, and the gray ones are the C atoms. The H atoms are omitted for clarity. The acetone molecules are stored in the hydrophobic space constructed by the *t*−butyl groups of ligands of Ru complexes drawn by the wireframe model.

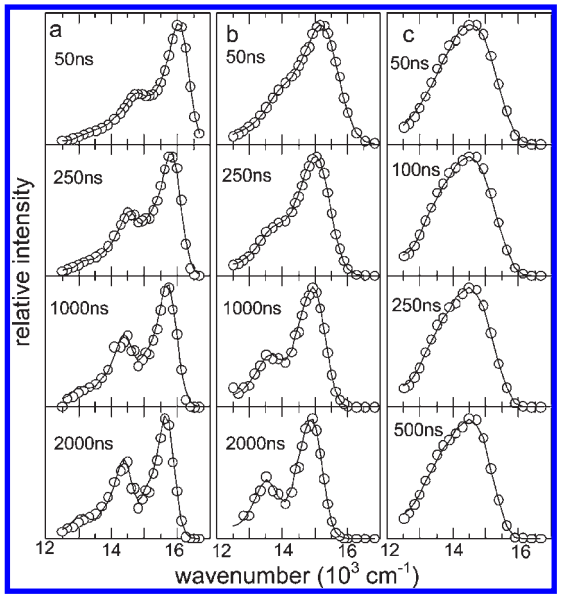

Figure 6. Time-resolved emission spectra of powdery: (a) $[Ru(dbb)_2(CN)_2]\cdot n CH_3OH$, (b) $[Ru(dbb)_2(CN)_2]\cdot 3(CH_3)_2CO$, and (c) $[Ru(dbb)_2(CN)_2]$ at 77K. Each spectrum is normalized to its maximum intensity. Open circles are experimental data and solid lines are results of the spectral fitting using the Franck−Condon analysis.

spectrum shift is not observed for $[Ru(dbb)_2(CN)_2]$ with no solvent of crystallization, as shown in Figure 6c. In the previous work about the transient emission of $[Ru(bpy)_2(CN)_2]$ in a fluid solution of ethanol−methanol at 130 K, a spectrum shift from 16 660 to 15 380 cm^{-1} was observed as a result of the solvent relaxation from the Franck−Condon state to the relaxed excited-state.[36] And the relaxation time in the solution was estimated as τ_r = 400 ns from the spectral shift against time. In the present work, we evaluated as τ_r = 1 250 ns for $[Ru(dbb)_2(CN)_2]\cdot n CH_3OH$ at 77 K. $[Ru(dbb)_2(CN)_2]\cdot 3(CH_3)_2CO$ was also examined in terms of the transient emission spectrum at 77K, and the peak shift from 15 280 to 14 960 cm^{-1} within 2000 ns was observed, as shown in Figure 6b. The relaxation time estimated as τ_r = 680 ns was shorter than that of $[Ru(dbb)_2(CN)_2]\cdot n CH_3OH$. Evidently, the higher the solvent Lewis acidity is, the larger the reorganizational energy in the excited state is, as has been discussed in refs 29 and 31 in the context of fluid solution.

The photoexcitation causes a decrease in the donor−acceptor interaction because the basicity at the CN ligand in the excited state is ca. 10^6 times smaller than that of the ground state.[37,38] Therefore, the local donor−acceptor interaction mainly contributes to the d_π (Ru) orbital energy via the Ru to CN back donation in the ground state.[29] Since each complex crystal includes several solvent molecules, we suggest that the solvent molecule close to the complex can interact with the CN ligands and control the 0−0 band energy of the MLCT transition. According to the X-ray crystallography of $[Ru(dbb)_2(CN)_2]\cdot 3(CH_3)_2CO$, the solvent molecule nearest to the pseudo-C_2 axis is considered as the most probable one to interact with the CN ligands. Although the distances (N1−C42 = 3.826 and N2−C42 = 4.807 Å) seem to be too far to interact the CN ligands with the acetone molecule, the emission spectrum, which is blue-shifted compared with the spectrum of $[Ru(dbb)_2(CN)_2]$ with no solvent molecule, suggests that the local donor−acceptor interaction is important. Analogously, the interaction for $[Ru(dbb)_2(CN)_2]\cdot n CH_3OH$ in the ground state is expected to be much larger, if its crystal structure is similar to that of $[Ru(dbb)_2(CN)_2]\cdot 3(CH_3)_2CO$.

We examined the contribution of dbb vibrations to the spectral profile using the Franck−Condon analysis on the medium- and low-frequency modes according to the literature.[39] The stretching vibration of dbb mainly contributes to the emission profile through the nonradiative decay from the ^{3}MLCT state because the ligand expands its framework in the excited state, where an electron is injected into the π^* orbital of the ligand. A spectral fitting for the transient emission spectra was carried out using the following equation:[39,40]

$$I(\tilde{\nu}) = \sum_{\nu_M=0}^{5}\sum_{\nu_L=0}^{5}\left(\frac{E_0 - \nu_M\hbar\omega_M - \nu_L\hbar\omega_L}{E_0}\right)^3\left(\frac{S_M{}^{\nu_M}}{\nu_M!}\right)\left(\frac{S_L{}^{\nu_L}}{\nu_L!}\right)\exp\left\{-4\ln 2\left(\frac{\tilde{\nu} - E_0 + \nu_M\hbar\omega_M + \nu_L\hbar\omega_L}{\Delta\tilde{\nu}_{1/2}}\right)^2\right\} \quad (1)$$

where S_M and S_L are the Huang−Rhys factors for medium- and low-frequency modes with $\hbar\omega_M$ and $\hbar\omega_L$, respectively. E_0 is the 0−0 band energy of the emission spectrum, and $\Delta\tilde{\nu}_{1/2}$ is the full width at half-maximum (fwhm) of a vibronic band. The S_M value is closely related to the reorganization energy (λ_M) in the ground state by the following equation:

$$\lambda_M = \frac{1}{2}k_M\Delta Q_M{}^2 = \hbar\omega_M S_M \quad (2)$$

(36) Kitamura, N.; Kim, H.-B.; Kawanishi, Y.; Obata, R.; Tazuke, S. *J. Phys. Chem.* **1986**, *90*, 1488.
(37) Peterson, S. H.; Demas, J. N. *J. Am. Chem. Soc.* **1976**, *98*, 7880.
(38) Davila, J.; Bignozzi, C. A.; Scandola, F. *J. Phys. Chem.* **1989**, *93*, 1373.
(39) Shinozaki, K; Shinoyama, T. *Chem. Phys. Lett.* **2006**, *417*, 111.
(40) Casper, J. V.; Westmoreland, T. D.; Allen, G. H.; Bradley, P. G.; Meyer, T. J.; Woodruff, W. H. *J. Am. Chem. Soc.* **1984**, *106*, 3492.

Table 3. Results in the Franck−Condon Analysis for the Ru Complex Crystals: (a) $[Ru(dbb)_2(CN)_2]\cdot n CH_3OH$, (b) $[Ru(dbb)_2(CN)_2]\cdot 3(CH_3)_2CO$, and (c) $[Ru(dbb)_2(CN)_2]$

	time, ns	E_0, cm^{-1}	$\hbar\omega_M$, cm^{-1}	S_M	λ_M, cm^{-1}	$\hbar\omega_L$, cm^{-1}	S_L	λ_L, cm^{-1}	$\Delta\tilde{\nu}_{1/2}$, cm^{-1}
a	50	16060	1360	0.46	620	650	0.46	290	670
	250	15850	1330	0.50	660	610	0.51	310	640
	1000	15730	1340	0.67	900	600	0.45	270	630
	2000	15670	1300	0.76	990	550	0.43	240	560
b	50	15280	1270	0.45	570	610	0.34	200	1100
	250	15120	1370	0.41	560	560	0.50	280	900
	1000	15030	1380	0.50	690	490	0.57	280	740
	2000	14960	1390	0.61	850	460	0.49	220	670
c	50	15510	1250	0.34	420	440	2.64	1160	600
	100	15480	1280	0.34	430	440	2.75	1210	580
	250	15390	1290	0.34	440	430	2.66	1130	560
	500	15280	1220	0.44	530	410	2.39	970	530

where ΔQ_M is a displacement of the nuclear coordinate between both the ground and excited states along the normal mode of the medium frequency, and k_M is the force constant. The best fits are shown as solid lines in Figure 6, and the parameters obtained by the least-squares method are listed in Table 3. For $[Ru(dbb)_2(CN)_2]\cdot n CH_3OH$, E_0 is gradually decreased in energy with time, while the vibrational energies of the medium frequency mode ($\hbar\omega_M$) at 50, 250, 1 000, and 2 000 ns are obtained at around 1 300 cm^{-1}, which is similar to the results in the same Franck−Condon analyses for other Ru complexes in solution reported before.[39,41−44] The Huang−Rhys factors (S_M) and the reorganization energy (λ_M) seem to be increased with time. For $[Ru(dbb)_2(CN)_2]\cdot 3(CH_3)_2CO$, the E_0's and λ_M's evaluated are slightly smaller than those of $[Ru(dbb)_2(CN)_2]\cdot n CH_3OH$, and the trends for S_M and λ_M are the same. This is accounted for by the difference in the ground-state donor−acceptor interaction between the two solvent-containing complex crystals. The value of $\hbar\omega_M$ represents the vibration of the bpy framework as well. For the dry complex crystal $[Ru(dbb)_2(CN)_2]$, the $\hbar\omega_M$'s are 1 200−1 300 cm^{-1}, and λ_M's are slightly smaller than those of the other crystals. The low-frequency modes also contribute to the nonradiative relaxation. The $\hbar\omega_L$'s and λ_L's are evaluated as 400−600 and 200−300 cm^{-1}, respectively, for both $[Ru(dbb)_2(CN)_2]\cdot n CH_3OH$ and $[Ru(dbb)_2(CN)_2]\cdot 3(CH_3)_2CO$. However, the reorganization energies (λ_L's) for $[Ru(dbb)_2(CN)_2]$ are relatively large.

Figure 7 is a schematic representation of the potential energy diagram relevant to the photorelaxation process. The donor−acceptor interaction of the Ru complex and the solvent molecules is represented as a curvature of the potential; it is deep in the ground state due to the strong interaction, while it is shallow in the excited state. Although the emission 0−0 band energy (E_0) is large at the earlier stage of the photorelaxation process, E_0 at the later stage is small because of the solvent molecule reorganization, depicted as the dotted arrow. The difference in the time-dependent E_0 for the crystals is also accounted for by the curvature of the ground state. Namely, the stronger the donor−acceptor interaction is, the larger the emission shift is. The evaluated λ_M and λ_L are considered to correspond to the difference between the Franck−Condon and the thermally equilibrated ground states in the diagram because the reorganization energy has

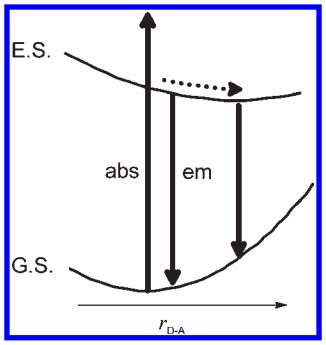

Figure 7. Schematic energy diagram for $[Ru(dbb)_2(CN)_2]\cdot n$(solvent) in the solid state. The local donor−acceptor interaction is represented in the potential curvature; that is, the excited-state potential curve is shallower than that in the ground state. The dotted arrow means the energy relaxation by the solvent reorganization in the excited state.

the contributions of the difference in solvent polarization and the internal structural change of the complex.[27]

We detected the luminescence vapochromism for the Ru complex in the solid state prepared as a thin film on a glass substrate in a sealed cuvette; the dark-red luminescence peaking at 740 nm of $[Ru(dbb)_2(CN)_2]$ with no solvent of crystallization turned bright orange (peaking at 640 nm) by the exposure to methanol vapor. The color change is accounted for by the sorption of methanol vapor in an analogy to the previous work for the $[Ru(dbb)_2(CN)_2]$−moisture system.[15] The luminescence color of the film is consistent with that of the $[Ru(dbb)_2(CN)_2]\cdot n CH_3OH$ crystal mentioned above. The bright orange luminescence was gradually darkened and red-shifted with evacuating the methanol vapor; namely, the complex solid released the sorbed methanol molecule in vacuum. The reversible luminescence color change was observed in the introduction−evacuation cycle of the methanol vapor. As shown in Figure 8, the emission spectrum was varied with the vapor pressure of methanol from 1.2 Pa to 12 kPa at room temperature; it was blue-shifted with increasing vapor pressure of methanol and vice versa.

The luminescence vapochromisms for other solvent vapors were observed as well. For example, benzene, quinoline, methylene chloride, and pyridine vapors gave emission peaking at 700, 660, 650, and 640 nm, respectively, at each vapor-pressure, P_{vap}, at 25 °C. Even the exposure to quinoline vapor with considerably low P_{vap} (< 100 Pa) showed the spectrum shift. The variation in the emission peak suggests that the complex has a discrimination capability for organic molecule vapors. The emission shift observed in the vapochromism is very similar to the "solvent effect" on the solid-state emission mentioned above. The vapochromism is elucidated as

(41) Kober, E. M.; Casper, J. V.; Lumpkin, R. S.; Meyer, T. J. *J. Phys. Chem.* **1986**, *90*, 3722.
(42) Kovács, M.; Horváth, A. *Inorg. Chim. Acta* **2002**, *335*, 69.
(43) Damrauer, N. H.; Boussie, T. R.; Devenney, M.; McCusker, J. K. *J. Am. Chem. Soc.* **1997**, *119*, 8253.
(44) Allen, G. H.; White, R. P.; Rillema, D. P.; Meyer, T. J. *J. Am. Chem. Soc.* **1984**, *106*, 2613.

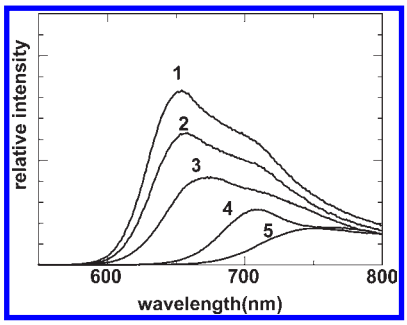

Figure 8. Luminescence spectra of $[Ru(dbb)_2(CN)_2]$ in a thin film under methanol vapor at P_{vap} = 12 kPa (1), 1.2 kPa (2), 120 Pa (3), 12 Pa (4), and 1.2 Pa (5) at room temperature.

follows. For the $[Ru(dbb)_2(CN)_2]\cdot 3(CH_3)_2CO$ crystal, the acetone stored in the hydrophobic space is unstable and easily desorbed from crystal. Therefore, a pore or hollow would be generated by the evacuation to prepare the solid film with no solvent of crystallization. When the film is exposed to organic vapor, the organic molecule is sorbed into the vacant space in the crystal. The local interaction between the CN ligands and the organic molecule causes the "solvent effect" of luminescence color. Consequently, it is possible to detect volatile organic compound (VOC) using the vapochromism of the $[Ru(dbb)_2(CN)_2]$ thin film based on the luminescence color as a function of reversibly entrained solvents of crystallization. Thin film or crystalline powder of the complex could, thus, be utilized not only for the VOC detection but also for molecular discrimination of organic vapors. This would be a novel function for VOC sensing, using an exceptionally stable and simple indicator.

Acknowledgment. This work was financially supported by the Ministry of Education, Science, Sports, and Culture for a Grant-in-Aid for Scientific Research (Grant 17550063) and Yokohama City University (Grants K18034 and K18002).

Supporting Information Available: The final results of X-ray crystallography of $[Ru(dbb)_2(CN)_2]\cdot 3(CH_3)_2CO$ is available as a CIF file. This material is available free of charge via the Internet at http://pubs.acs.org.